A FUSION DESIGN STUDY OF NONMOBILE BLANKETS WITH LOW LITHIUM AND TRITIUM INVENTORIES

REACTORS

KEYWORDS: *design, breeding blankets, thermonuclear reactors, lithium, tritium, inventories, beryllium, helium, coolants, thermonuclear reactor materials, stainless steels*

MOHAMED A. ABDOU *Argonne National Laboratory*
Applied Physics Division, Argonne, Illinois 60439

LAYTON J. WITTENBERG *Monsanto Research Corporation*
Mound Laboratory, Miamisburg, Ohio 45342

CHARLES W. MAYNARD *University of Wisconsin*
Nuclear Engineering Department, Madison, Wisconsin 53706

Received December 30, 1974
Accepted for Publication March 24, 1975

Developing a controlled thermonuclear reactor blanket that minimizes lithium and tritium inventories is feasible. The tritium inventory is minimized by keeping the lithium inventory to a minimum and utilization of a lithium-bearing compound with low retention for tritium and an efficient tritium extraction system. The lithium inventory is minimized by employing a thin layer of ^6Li operating in a soft neutron spectrum obtained by slowing down the deuterium-tritium (DT) neutrons in beryllium. Material properties and performance such as tritium retention, irradiation characteristics, and chemical compatibility of possible lithium-bearing materials and beryllium compounds have been evaluated. The blanket of the conceptual fusion reactor UWMAK-II uses stainless steel for first wall and structure, helium coolant, lithium aluminate enriched to 90% ^6Li for tritium breeding, metallic beryllium for neutron multiplication and moderation, and graphite for reflection and additional neutron moderation. A breeding ratio of 1.18 and nuclear heating of 18 MeV per DT neutron are obtained. The lithium inventory is only 4×10^4 kg (40 Mg). The steady-state inventory of tritium in the breeder is only 40 g, which is more than two orders of magnitude lower than that in blankets using lithium for cooling and neutron moderation as well as tritium breeding. Tritium leakage to the steam is kept to ~1 Ci/day by oxidation of the tritium in the helium coolant and absorption by a molecular sieve dessicant. Plant reliability is improved and accidental tritium and energy release are minimized in the type of blankets examined in this study.

I. INTRODUCTION

Current fusion reactor designs, based on the deuterium-tritium (DT) fuel cycle, that utilize liquid lithium as the breeding material, coolant, and neutron moderator, typically[1-3] employ lithium regions of 40- to 70-cm thickness. The lithium must circulate at high flow rates from the blanket to external equipment for heat and tritium removal. This circulation of lithium introduces disadvantages associated with corrosion and magnetohydrodynamic conversion (MHD) pumping effects, and requires a significant amount of lithium outside of the blanket. Although the proposed but untested extraction systems maintain low tritium concentrations (<5 ppm), the total amounts of tritium are large (up to 9 kg) because of the large lithium inventories. For the same tritium breeding ratio, minimizing the amount of lithium[4] can ease the requirements on the design of the tritium extraction system, decrease the total tritium inventory, and lower the total energy and tritium that would be released in the event of such accidents as lithium fires. Consequently, blanket designs with low lithium and tritium inventories are examined in this study.

The mean-free-path for a tritium-producing reaction, λ_t, in natural lithium, is more than 70 cm for a 14-MeV neutron while it is only 2 cm for a 1-eV neutron. Significant reduction in lithium inventory is possible, therefore, only if the lithium region is operated in a neutron flux possessing a soft energy spectrum. Since the threshold for the $^7Li(n,n'\alpha)T$ is 2.8 MeV, the presence of ^7Li becomes a disadvantage if the neutron energy spectrum is shifted appreciably toward low energies as it merely lengthens λ_t. Pure ^6Li is expensive, however, and we limit the

designs here to lithium enriched to 90% in ^{6}Li. The λ_t in this case is ~0.15 cm for 1-eV neutrons and only 3- to 5-cm-thick lithium layers are required to absorb almost all low-energy neutrons in tritium-producing reactions.

A system highly enriched in ^{6}Li requires, however, the use of a neutron multiplier to have a tritium breeding ratio of >1 because of unavoidable parasitic absorption in the first wall and structural components. The neutron multiplier must have (a) a large $(n,2n)$ cross section, (b) a low threshold for the $(n,2n)$ reaction to increase (or at least minimize the loss in) energy multiplication, and (c) a small parasitic capture cross section. Beryllium is the only material that has these characteristics and that must be utilized in the blanket if the use of fissionable materials is excluded.

Blankets with low lithium inventories continue to require high velocities for circulation of the lithium from the blanket for tritium removal.[5] The disadvantages associated with the circulation of lithium or a lithium-bearing fused salt are avoided if the breeding material remains stationary in the blanket region and the tritium is removed continuously by appropriate methods. As a result, solid breeder materials can be considered.[6,7] These solids will improve the plant reliability because a first-wall rupture in this case will not result in a liquid breeder material leaking into the plasma region.

Based on the above discussion, a controlled thermonuclear reactor (CTR) blanket with low lithium and tritium inventories in a solid breeding material appears to offer several advantages from plant reliability and safety considerations. Therefore, these blankets are examined in greater detail in this paper. Potential materials for these blankets are described in Sec. II. The neutronic characteristics of these blankets are discussed in Sec. III. Finally, in Sec. IV, a detailed description of one complete system is given, and the conclusions of this study are presented in Sec. V.

II. MATERIAL CONSIDERATIONS

Nonmobile breeder blankets require that a number of materials be examined as blanket constituents along with their physical arrangement within the blanket. The blanket constituents can be classified according to their function, namely: coolant, structure, neutron multiplier, neutron moderator, and tritium breeder. The ultimate choice of a material for each function will depend on its neutronics behavior, potential radiation damage, physical properties at operating temperatures, and compatibility with other components. Also, each component must be compatible with the operations of the tritium removal system in which the tritium may exist in molecular or atomic form, or as tritium oxide.

II.A. Coolants

The potential coolants for fusion designs can be classified into two physical states: gaseous and liquid. The gaseous coolants that may be considered are the permanent gases, chiefly helium, the metallic vapors, carbon dioxide, and perhaps steam. The liquid coolants that may be considered are water, high-boiling organic compounds, liquid metals, and fused salts. Water is limited in its usefulness because of its low critical temperature, 375°C. Also, the unknown radiation stability of the organic liquids make their use less certain at this time. Carbon dioxide is not compatible with most CTR materials. In addition, it is difficult to separate tritium from this gas.

Based on presently developed technology, the choice of a coolant lies among helium, a liquid metal, or a fused salt. Each of these fluids must be circulated at rather high flow rates from the blankets to the external equipment for heat and/or tritium removal. The ability to transport tritium can be one determining factor in the choice of a coolant. Also, the MHD pressure associated with pumping conducting fluids across magnetic flux lines must be overcome by judicious design of the fluid flow channels or the development and utilization of nonconducting tubing.[8] Simpler flow designs are possible, therefore, if helium is utilized, and chemical compatibility problems are reduced by the use of this inert gas. In addition, the neutronics interactions with helium are insignificant, except for the ~200 ppb (Ref. 9) of ^{3}He which would be rapidly transmuted in an operating reactor; consequently, the utilization of helium does not perturb the neutronic behavior of the proposed blankets. For the reasons cited, helium is chosen as the coolant for this study.

II.B. Structure

The blanket structural materials suggested in various reactor studies are: aluminum, stainless steel, niobium, vanadium, and molybdenum alloys.[10] The choice of the structural material depends on the fusion design parameters and on the proposed operating temperatures. Aluminum appears limited in usefulness because of its low melting point, 660°C, unless special arrangement is made to preferentially cool the aluminum structure. Excessive oxidation of niobium, and probably vanadium, alloys are predicted[11] in even

extremely pure helium, while the behavior of molybdenum is not well known. Based on this cursory examination, stainless steel was selected as the structural material for this study, although vanadium, which has a single isotope, is considered in most cases of the neutronic parametric study presented in Sec. III. The maximum temperature of the stainless-steel structure is limited to ~600°C by tensile strength considerations.[1]

II.C. Neutron Multipliers

The incorporation of beryllium in a nonhybrid blanket of highly enriched lithium is necessary to have a tritium breeding ratio of >1. The chemical form of the beryllium in the fusion reactor can be either a metallic or a stable compound, such as BeO or Be_2C. A number of high melting intermetallic compounds[12] with compositions, MBe_{12} and MBe_{13}, are formed, but information on their behavior is insufficient for their consideration at this time. The physical properties of each material (Table I), their neutronic behavior, irradiation characteristics, and chemical compatibility must be considered.

The important neutronic reactions of beryllium are the $(n,2n)$, the (n,α), and (n,T) reactions. These reactions generate nearly 8 cm^3 (STP) helium and 3.3×10^{-2} cm^3 (STP)T_2 per cm^3 Be (metallic) per year per (MW/m^2) in a reference Tokamak design (see Sec. IV). The corresponding formation of T_2 and helium in BeO is approximately proportional to the beryllium density; however, utilization of BeO has a detrimental effect on neutron production, as discussed in Sec. III.

The irradiation behavior of beryllium and BeO can be estimated based only on experimental data collected in fission reactors. However, in fission irradiation the total helium production has been only 0.5 cm^3 (STP) helium/cm^3. At this level of irradiation, Weir[17] found that the helium was insoluble in the metal and was collected as bubbles at nucleation sites. No swelling of the metal occurred under 600°C. Above 600°C, swelling increased with temperature and reached ~0.5% at 700°C and 1.5% at 750°C. These results are only 25% of the predicted swelling values.[17] At similar fluences, the stress-rupture values for beryllium tubing decreased nearly 30% at 600°C. This information indicates that in a fusion reactor blanket operating near 600°C, the beryllium metal could not be used as a structural member but must be supported in such a manner as to accommodate 10 to 30 vol% swelling per year.

The escape of helium from BeO compacts has been measured during irradiation at several temperatures by Carteret et al.[18] The ratio of R/B, where

R = quantity of helium released from the solid in unit time

B = quantity of helium formed in unit time,

tended to become a constant, less than one, at each temperature after an initial induction period. For instance, R/B increased from 0.12 at 1020°C to 0.19 at 1350°C. These results were interpreted to mean that helium release is due partly to the diffusion of interstitial helium atoms, but that most of the helium nuclei remained in substitutional position. Because the helium atom is larger than the octahedral position in a BeO lattice, the interstitial helium atoms would presumably lead to expansion of the compacts. Swelling would be predicted to be especially important below 1000°C, where the helium release is probably small. Unfortunately, density changes were not measured on these compacts. Density changes for BeO single crystals have been obtained during irradiation in the 390°C temperature range. Hickman and Walker[19] found that the expansion was highly anisotropic, that it decreased with temperature, and that it was ~0.15% at 550°C. Based on this information, the volume expansion for BeO in a fusion reactor would be at least 1.5% in 1 yr.

Although the quantity of tritium produced in beryllium is small, the fate of this tritium in both beryllium and BeO is of importance. Apparently, BeH_2 cannot be formed by direct combination of the elements.[20] The solubility of tritium in beryllium has been reported[21] to be small, $\sim 7.6 \times 10^{-3}$ $cm^3/(g\ atm^{1/2})$ at 900°C; consequently, when the tritium pressure is maintained below 10^{-4} Torr, only 1 g of tritium is dissolved in the total blanket of beryllium described in Sec. IV. The diffusion of tritium in beryllium, 4.6×10^{-8} cm^2/sec at 900°C, suggests that diffusion path lengths as long as 450 μm would delay the diffusional release of

TABLE I

Potential Neutron Multipliers

Material	Melting Point (°C)	Boiling Point (°C)	Beryllium Atoms ($10^{22}/cm^3$)
Be[a,b]	1283	2483	12.3
BeO[c]	2520	4260	7.3
Be_2C[d]	2400	2530	9.8

[a] Ref. 13.
[b] Ref. 14.
[c] Ref 15.
[d] Ref. 16, pp. 67-69.

tritium by only 1 g for the total reactor. Conversely, the diffusional release of tritium from irradiated BeO has been measured and found to be very slow[22] (Fig. 1), $\sim 10^{-15}$ cm^2/sec at 900°C. As a consequence, the longest diffusion path in a BeO compact must be <1 μm in length if the inventory of the tritium in the BeO is to be kept below 100 g per reactor. Both beryllium and BeO should be utilized as particles, therefore, in the appropriate size range.

The chemical compatibility of BeO with stainless steel at high temperature should be excellent because of its high heat of formation compared on a per-mole-of-oxygen basis with the oxides of the elements in the steel.[23] Conversely, beryllium was found to be incompatible with stainless steel because of the rapid formation of the intermetallic compound, $FeBe_{13}$, at 600°C in vacuum. At the same temperature and pressure, the experimental work of Vickers[24] suggests that the stainless steel can be protected by a protective layer of sintered Al_2O_3 or ZrO_2, such as might be applied by plasma spraying techniques.

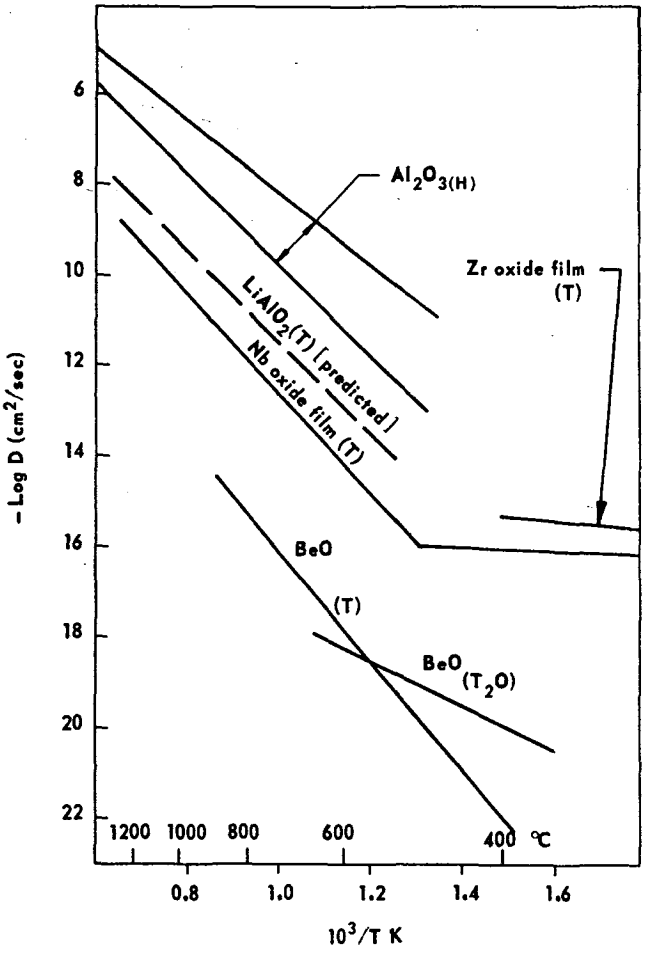

Fig. 1. Diffusion of tritium or hydrogen in ceramic materials.

II. D. Breeder Materials

The lithium compound selected as the tritium breeding material must satisfy many requirements. It must have properties exhibited by the other blanket constituents, such as desirable neutronics and irradiation characteristics, chemical stability at operating temperatures, and compatibility with the other blanket materials. In addition, the lithium compound must breed and release tritium. Any compound selected will eventually release tritium at the rate at which it is formed; however, the release must be at a rate sufficiently high that the tritium inventory in the blanket is not excessive. Further, since nearly 50% of the nuclear heating is generated in the lithium region, the temperature of the lithium material, depending on its thermal conductivity, can greatly exceed the average temperature in the blanket. Several classes of compounds are suggested, namely metallic, salts, and ceramic (see Table II). The most likely candidates in each class are examined next in greater detail.

II. D. 1. Lithium

Liquid lithium contained in steel capsules might be a potential breeder component. Tritium removal from sealed capsules is limited, however, because of the low permeability of tritium in

TABLE II

Potential Nonmobile Breeder Materials

Material	Melting Point (°C)	Vapor Pressure	Lithium Atoms (10^{22}/cm^3)
(Metallic)			
Li (liquid)[a]	180	1342°C (boiling point)	4.2
Li Al[b]	718	---	2.7
Li_3 Bi[b]	1145	---	4.0
(Nonmetallic)			
Li_2O[c]	1700	10^{-1} Torr (1400°C)	8.2
LiOH[c]	471	5 Torr H_2O (500°C)	3.7
$LiAlO_2$[d]	1700	Li_2O (1400°C)	2.3
Li_4SiO_4[e]	1256	Li_2O (1256°C)	4.8
Li_2C_2[f]	>1000	Li (1000°C)	4.1
LiF[g]	848	boiling point (1693°C)	6.1
LiH[a,c]	686	24 Torr H_2 (686°C)	5.9

[a] Ref. 25.
[b] Ref. 12.
[c] Ref. 26
[d] Ref. 27.
[e] Ref. 28.
[f] Ref. 16, pp. 61-63.
[g] Ref. 29.

stainless steel and the high solubility of tritium in the lithium. For instance, to keep the tritium inventory below 1 kg in the blanket of the design proposed in Sec. IV, the liquid lithium would need to be encapsulated in nearly 10^{10} steel cylinders with a diameter of only 0.6 mm and a wall thickness of 0.1 mm. The utilization of such capsules is impractical.

Distillation of tritium from the lithium by the use of a porous plug in the capsule might be considered also; however, such a technique is not feasible because of the azeotropic solution which is predicted at low tritium concentrations.[30] As a result, the vapor phase would be richer in lithium, and tritium would concentrate in the capsule.

II.D.2. Intermetallic Compounds

Lithium forms intermetallic compounds melting above 600°C with aluminum, bismuth, lead, silicon, and tin. While some of these compounds may be useful in specialized blanket designs, the radiation stability of these compounds and the effects of the alloying elements on the neutronic behavior of the blankets must be determined.

A major drawback to the utilization of the intermetallic compounds is the appearance of liquid phases at much lower temperatures as the lithium atoms are transformed by nuclear reactions. For instance, when lithium in the high melting compound Li_3Bi (1145°C) is transmuted by nuclear reactions, the bismuth composition increases so that a liquid phase is formed at 415°C by a peritectic reaction mechanism. This liquid would promote sintering of any discrete particles and radically decrease the rate of tritium release.

The compound LiAl (melting point, 718°C) exhibits a wide solid solubility region[12]; the melting temperature, 718°C, would be lowered only ~10°C by the transmutation of the lithium atoms after 2 yr of neutron irradiation. While the lowering of the melting temperature does not limit the usefulness of this compound, the effect of sintering does, because rapid sintering of metallic alloys occurs at approximately one-half times the melting temperature (in K); therefore, discrete particles of this alloy above 150°C would sinter, form a large mass, and increase the diffusional paths for tritium release.

II.D.3. Nonmetallic Compounds

An initial survey of these compounds indicates that the oxide-bearing ceramics have the highest melting points (Table II), except for the carbide, which will be discussed later. The compound Li_2O has a high melting point and a high lithium atom density, although its vapor pressure prohibits its use above ~1400°C. The chemical properties of the monoxide are poorly suited for its large-scale usage, however, because of its strong affinity for water and carbon dioxide.[29] The reaction

$$Li_2O + H_2O = 2LiOH$$

has a free energy change of -22.7 kcal at 298 K; consequently the equilibrium vapor pressure of H_2O at 298 K is $\sim 10^{-14}$ Torr, and the dry powder would be impossible to fabricate in even the driest glove box. Instead, the blanket modules would be fabricated using LiOH, which must be dehydrated at elevated temperature after assembly. This dehydration procedure would be very difficult for a large blanket and would be made more difficult by the need to remain below the melting point of the hydroxide, 471°C.

Lithium oxide forms compounds with Al_2O_3 and SiO_2, which have much lower affinity for carbon dioxide and water; consequently, these compounds could be fabricated in dryboxes. In the Li_2O-Al_2O_3 system,[27] only two compounds exist, $LiAlO_2$ and $LiAl_5O_8$. The melting point of the lithium-rich compound, $LiAlO_2$, has been reported between 1610 and 1700°C. Such determinations were difficult because of the vaporization of lithia, which began at ~1400°C, and which caused a change in the composition of the sample. A eutectic liquid reported at ~1670°C between the compounds Li_2AlO_2 and $LiAl_5O_8$ would form as the lithium in the compound $LiAlO_2$ is transformed by neutron irradiation. The appearance of this liquid, the vaporization of lithia, and the sintering of ceramic compounds, which becomes rapid at 0.8 of the melting point,[31] probably limits the usefulness of this compound to ~1300°C.

Lithium orthosilicate, Li_4SiO_4, and metasilicate, Li_2SiO_3, are stable compounds[28] that may be useful. The orthosilicate has a high lithium atom density, a lithium content per gram-formula weight greater than the metasilicate or the aluminates, and it is nonhygroscopic. However, the orthosilicate melts, by a peritectic reaction with Li_2O at 1255°C, and the rapid vaporization of lithia at this temperature has been reported. Also, as the lithium in the orthosilicate transforms as a result of neutron irradiation, a eutectic liquid forms at 1024°C between the ortho- and metasilicates; consequently, the useful temperature limit of the orthosilicate is <1000°C.

In addition to the oxide ceramics, the carbide of a metal is often a stable compound. Lithium forms a single carbide, Li_2C_2, which reacts readily with water to yield actylene. Although the detailed crystal structure of this compound has not been reported, it probably exists as a salt in which the carbon atoms form a dimer, similar to CaC_2, so that it is not a stable high-temperature compound. This behavior was demonstrated in the

study of the Li-Li_2C_2 system[16] in which the trend of the melting point data indicated the melting point of Li_2C_2 would be much greater than 1000°C; however, at temperatures >800°C in a vacuum, the lithium readily vaporized. The study also reported polymorphic transformation temperatures at 410, 490, and 560°C, which may limit its usefulness to even lower temperatures.

The lithium halide salt, LiF, has a high lithium atom density but its relatively low melting and boiling points probably limit its usefulness. Also, the tritium, which is generated in a fluoride salt, would probably be released as molecular TF, which can cause potentially serious corrosion problems if released into the helium coolant channels; consequently, a low-temperature fused salt mixture would have to be circulated to external equipment for removal of the TF, as has been proposed previously.[32]

Lithium hydride (or deuteride) has many desirable neutronic characteristics as a potential tritium breeding material or neutron moderator. Its low melting point and high hydrogen pressure (Table II) pose serious limitations on its usefulness, however. These undesirable characteristics might be overcome by clever design of the blanket modules and the accompanying tritium extraction system.

II. D. 4. Tritium Release Considerations

The lithium compound used in the blanket must not only have desirable physical properties, as previously discussed, but it must also release the tritium readily so that the total tritium inventory is acceptable. For any lithium compound, a steady state will be approached in which the rate of tritium release will equal the generation rate; consequently, the factors that affect this steady-state condition are of importance. The rate of approach to the steady-state condition is dependent on kinetic considerations, such as the diffusion of tritium in the lithium compound, while the thermodynamic equilibrium is determined by the solubility of the tritium in the lithium compound at a given temperature and tritium partial pressure in the recovery system. Both diffusion and solubility need to be considered, therefore, for each lithium-bearing material.

When liquid lithium was utilized as a breeder and coolant, for instance, the rate of diffusion of the tritium in the lithium was not important because mechanical agitation would quickly redistribute the tritium. The important consideration in that case was the partial pressure of tritium in the recovery system and the equilibrium solubility of tritium. It was necessary to employ a recovery system which had a tritium partial pressure of $<10^{-10}$ Torr to keep the solubility <5 ppm (wt), which gave a tritium inventory of nearly 9 kg.

For the solid lithium-bearing compounds considered in this study, the tritium diffusion will not be as rapid as is the case for liquid lithium. The relationship between the tritium concentration in a solid breeder material and its diffusion coefficient in that same solid can be evaluated approximately by use of Jost's solution[33] to the problem of the photochemical generation of a gaseous molecule in a cylindrical vessel with the corresponding diffusion of the molecule to the walls of the cylinder where their concentration is zero. For this case, the average concentration of the generated species, $\overline{C}$, is given by the equation

$$\overline{C} = \frac{T\,\delta^2}{3\,D} \quad ,$$

where

T = tritium generation rate

δ = path length (radius of cylinder)

D = diffusion coefficient.

This relationship will be used to evaluate the average tritium concentration in several solid breeder blankets for a reactor of the size described in Sec. IV, in which T is 10^{-2} g/sec. If the tritium in the intermetallic compound LiAl is in solid solution, and if the interstitial diffusion is similar to the diffusion of hydrogen in common metals, then $D \approx 10^{-5}$ to 10^{-6} cm^2/sec. For particles with $\delta \approx 10^{-1}$ cm, the total tritium holdup in the blanket due to diffusion is ~15 g.

For this same compound, LiAl, an estimation of the solid solubility of tritium has been made based on the assumption that a Sieverts' relationship exists. Recent experimental measurements, regarding the release of tritium from irradiated LiAl pellets at temperatures from 300 to 600°C and concentrations in the range of 1 appm, indicate that the Sieverts' constant at 500°C is no larger than 2×10^7 Torr/(atom fraction)^2. If the tritium pressure is kept below 10^{-4} Torr, for a reactor of the size described in Sec. IV, the approximate tritium solubility in a LiAl blanket is only 130 g. It can be seen that the tritium solubility in LiAl is the predominant effect in the accumulated tritium inventory as compared to the holdup by diffusion when particles <0.1 cm are utilized.

The diffusion and solubility of tritium in the nonmetallic compounds are more difficult to estimate because very few measurements have been published on these properties of ceramic materials with either hydrogen or tritium. If the diffusion of tritium in $LiAlO_2$ is similar to the diffusion of hydrogen in Al_2O_3, for instance, then

the measured values for this latter system can be used, although wide variations exist between the two reported experiments[34,35] (Fig. 1). Also, in the few cases where tritium diffusion has been measured in zirconia, beryllia, and niobia,[36] the apparent diffusion coefficients are much lower than for Al_2O_3. Although this difference may truly reflect enhanced diffusion of hydrogen in alumina, a difference in experimental techniques should be noted. In the measurements on alumina, a differential hydrogen pressure was maintained across a ceramic specimen; consequently, any porosity in the specimens would contribute to an apparently higher diffusion coefficient. In the experiments involving tritium, the tritium was either generated within the specimens or injected by nuclear recoil energy. The diffusion measurements were conducted as the tritium migrated to the surfaces of the specimens and probably followed lattice diffusion paths more closely than the hydrogen gas permeation experiments of alumina. Higher diffusion coefficients have been reported[37] for tritium or hydrogen in UO_2, ZnO, and TiO_2; however, the structures of some of these compounds provide easy paths for tritium diffusion. For all of these reasons, a conservative diffusion rate for tritium in $LiAlO_2$ or Li_2SiO_4 is proposed, as shown in Fig. 1.

In the experimental determination of the effusion of tritium from beryllia particularly below 750°C, an appreciable amount of molecular T_2O was evolved. The release of T_2O followed a faster diffusion rate at the lower temperatures, as shown in Fig. 1; however, T_2O represented only 3% for polycrystalline materials and 12% for single crystals of the total tritium released. This information indicates that tritium oxide will be released together with molecular tritium from all of the oxide-bearing breeder compounds and requires that the tritium recovery system be capable of processing both T_2 and T_2O.

The solubility of hydrogen, S, as a function of temperature and pressure has been measured for only one oxide, ZnO, and found to be very small.[38] The data, which followed a Sieverts' relationship with square root pressure dependency at low hydrogen pressure, are represented approximately by the equation

$$S = \left(2.1 \times 10^6 \frac{\text{cm}^3}{\text{cm}^3 \cdot \text{atm}^{1/2}}\right) \cdot \times \exp\left(-\frac{36.7 \times 10^3}{RT} \text{ cal/mole}\right) .$$

Based on chemical considerations, Hickman[37] suggests that ZnO is a more receptive host for hydrogen than alumina. One would predict, therefore, that the solubility of tritium in an aluminate or silicate should be no greater than the solubility of hydrogen in ZnO, so that the latter data can be used as a maximum value.

II. D. 5. Irradiation Behavior of Ceramic Compounds

The tritium and hydrogen diffusion and solubility data for ceramic materials and the phase diagrams, previously discussed, were obtained on unirradiated materials. In a fusion reactor blanket, however, these materials will be subjected to high fluxes of energetic neutrons, alpha and tritium recoil particles, and large accumulations of helium; consequently, the properties of the unirradiated materials can be changed significantly. An estimation of their irradiation behavior is therefore necessary.

Early work on the neutron irradiation of ceramic materials at fluences of $\sim 10^{19}$ n/cm^2 indicated good irradiation stability. Fast fission irradiation[39] ($\sim 10^{20}$ n/cm^2) produced volume expansions that were removed by anneals above 400°C. When these ceramic materials were irradiated with fission fragments or alpha-particles, severe radiation damage of many ceramics occurred.[40] The anisotropic materials, such as Al_2O_3 and $ZrSiO_4$, were especially susceptible to damage and formed a quasi-amorphorous (metamictic) material during low-temperature irradiation. Matzke and Whitton[41] produced the same type of radiation damage in ceramic materials by ion-bombardment with inert gas atoms. They showed, however, that the crystalline character of the specimens returned when annealed above 0.4 of the melting temperature, which was 600 to 700°C for alumina. The inert gases were nearly quantitatively released at these same temperatures. If lithium aluminate behaves similarly, then its irradiation temperature should be kept above 600°C so that the well-defined crystalline structure of the material is maintained. Above this temperature, the helium release should proceed so that the release rate becomes a significant fraction of the generation rate, as was previously discussed for BeO. More importantly, in the annealed lattice the tritium diffusion and solubility should be similar to the behavior of unirradiated materials.

III. NEUTRONICS ANALYSIS

As explained in the introduction, to minimize the lithium inventory in CTR blankets it is necessary to use highly enriched lithium and beryllium. Clearly, employing a large amount of beryllium allows significant reduction in the lithium volume. However, the magnitude of beryllium reserves and

resources is not well known at present. The known resources[42] of the U.S. are believed to be limited to 2×10^4 ton. An 8-cm-thick layer of beryllium in a toroidal reactor with minor and major radii of 5 and 13 m consumes ~2% of these resources. Thus, the question of beryllium resources needs to be investigated thoroughly, since it is crucial for minimizing the lithium inventory in CTR blankets in addition to its well-recognized importance for increasing energy multiplication in almost all conceptions of fusion blankets.[3] Indications are that world prospective resources may be larger than 0.6×10^6 ton. If this proves to be true, then a few hundred fusion reactors can utilize moderate amounts of beryllium without exhausting a large fraction of the reserves. In any event, a prudent neutronics design at present should minimize the amount of beryllium incorporated into CTR blankets.

Several lithium and beryllium compounds were discussed in the previous section from material considerations rather than neutronics. In this section, we evaluate the neutronics behavior of most of these compounds.

Table III describes several designs for which the neutronics analysis was carried out. One-dimensional cylindrical geometry with a plasma radius of 250 cm and an inner first-wall radius of 300 cm was assumed. All the neutron and gamma-ray transport calculations were carried out with the ANISN program[43] in the S_8-P_3 approximations. All neutron and multigroup cross sections were

TABLE III

Description of Several Designs with Low Lithium Inventory for Which Neutronics Analysis Was Carried Out

Zone[a]	Design 1		Design 2		Design 3		Design 4	
	t[b]	Composition[c]	t	Composition	t	Composition	t	Composition
3	1	vanadium	1	vanadium	1	vanadium	1	vanadium
4	5	90% Be + 10% V	1	90% Li + 10% V	1	90% Li + 10% V	1	90% Li + 10% V
5	5	90% Be + 10% V	10	90% Be + 10% V	5	90% Be + 10% V	5	90% Be + 10% V
6	2	90% Be + 10% V	2	90% Be + 10% V	2	90% Be + 10% V	0.0	---
7	2	90% Li + 10% V	2	90% Li + 10% V	2	90% Li + 10% V	2	90% Li + 10% V
8	2	90% Be + 10% V	2	90% Be + 10% V	2	90% Be + 10% V	0.0	---
9	57	graphite	57	graphite	57	graphite	57	graphite

Zone[a]	Design 5		Design 6		Design 7	
	t	Composition	t	Composition	t	Composition
3	1	vanadium	1	vanadium	1	vanadium
4	1.5	90% Li + 10% V	1	90% $Li_2Al_2O_4$ + 10% V	1	90% Li_2O + 10% V
5	5	90% Be + 10% V	5	90% Be + 10% V	5	90% Be + 10% V
6	0.5	90% Li + 10% V	0.0	---	0.0	---
7	2	90% Li + 10% V	2	90% $Li_2Al_2O_4$ + 10% V	2	90% Li_2O + 10% V
8	0.5	90% Li + 10% V	0.0	---	0.0	---
9	57	graphite	57	graphite	57	graphite

Zone[a]	Design 8		Design 9		Design 10	
	t	Composition	t	Composition	t	Composition
3	1	vanadium	1	vanadium	1	stainless steel
4	1	90% $Li_2Al_2O_4$ + 10% V	1	90% LiAl + 10% V	1	90% $Li_2Al_2O_4$ + 10% SS
5	5	90% BeO + 10% V	5	90% Be + 10% V	5	90% Be + 10% SS
6	2	90% BeO + 10% V	0.0	---	0.0	---
7	2	90% $Li_2Al_2O_4$ + 10% V	2	90% LiAl + 10% V	2	90% $Li_2Al_2O_4$ + 10% SS
8	2	90% BeO + 10% V	0.0	---	0.0	---
9	57	graphite	57	graphite	57	graphite

[a] In all designs: Zone 1 (central section of the cylindrical geometry) is the plasma region with an outer radius of 250 cm; and zone 2 is a vacuum gap of 50 cm.

[b] The t is the thickness of the zone in cm.

[c] All composition percentages are by volume and lithium is enriched to 90% in ^6Li in all designs except design 5 for which lithium is enriched to 60%.

processed using the SUPERTOG code[44] and SMUG code[45] from ENDF/B-III data.[46] The gamma-ray production cross sections were processed from ENDF/B-III with the LAPHANO code.[47] Neutron kerma factors and partial group cross sections were processed with the MACK code[48] from ENDF/B-III. The energy group structure used in all cases consists of 46 neutron groups and 43 gamma-ray groups.[49]

All the designs described in Table III have the common feature of low lithium inventory, i.e., the total thickness of the lithium region is <5 cm. Design 2, as shown schematically in Fig. 2, consists of a 1-cm vanadium first wall, a 1-cm region of 90% lithium plus 10% vanadium, a 12-cm-thick region of 90% metallic beryllium plus 10% vanadium, and regions consisting of 2 cm of 90% lithium plus 10% vanadium, 2 cm of 90% beryllium plus 10% vanadium, and 57 cm of graphite. All composition percentages in Table III are by volume. Design 1 is the same as design 2 except the 1-cm lithium-vanadium region behind the first wall is removed. The amount of beryllium is decreased from 14 cm in design 2 to 9 cm in design 3 and 5 cm in design 4. All designs except design 5 utilize lithium enriched to 90% in ^{6}Li. The effect of reducing the lithium enrichment from 90 to 60% ^{6}Li, but using roughly the same optical thickness of ^{6}Li as in design 4, is shown by design 5. Designs 4, 6, 7, and 9 compare the performance of lithium, $Li_2Al_2O_4$, Li_2O, and LiAl, respectively. Design 8 is the same as design 6 but metallic beryllium is replaced with beryllium oxide with approximately the same amount of beryllium. Vanadium is employed as the first wall and structure in designs 1 through 9. The effect of stainless steel is brought up in design 10, which is obtained by 1-to-1 volume substitution of stainless steel for vanadium in design 6.

Table IV summarizes the most important neutronics results for the designs described in Table III. Comparing the neutronics results for designs 2, 3, and 4 we find that the tritium breeding ratio and energy multiplication are quite sensitive to the amount of beryllium. These three designs employ 2.7 cm of 90% enriched lithium, and ~5 cm of beryllium is the minimum for such designs to have a tritium breeding ratio of ~1.15. The tritium breeding ratio and energy per fusion reaction increases rather rapidly as the amount of beryllium is increased up to ~8 cm; then the rate of increase becomes slower as additional amounts of beryllium are employed. It can also be seen from Table IV, design 1, that the removal of the 1-cm enriched lithium layer behind the first wall in design 2 causes the tritium breeding ratio to drop by more than 35% despite the 5% increase in the Be(n,2n) reaction rate. The energy production, however, increases by ~2 MeV per DT neutron. The reason for this can be explained by the strong competition of the V(n,γ) with the ^{6}Li(n,α)t reaction in a neutron spectrum greatly softened by the Be(n,2n) reaction. The angular distribution of the secondary neutrons emerging from the Be(n,2n) reaction is nearly isotropic and, therefore, a large fraction of these neutrons stream back in the direction of the first wall. The removal of the ^{6}Li layer from behind the first wall increases the capture rate in vanadium from 0.2 to 0.6 reactions per DT neutron. The Q-value for the V(n,γ) reaction is ~50% larger than the Q-value in the ^{6}Li(n,α)t reaction.

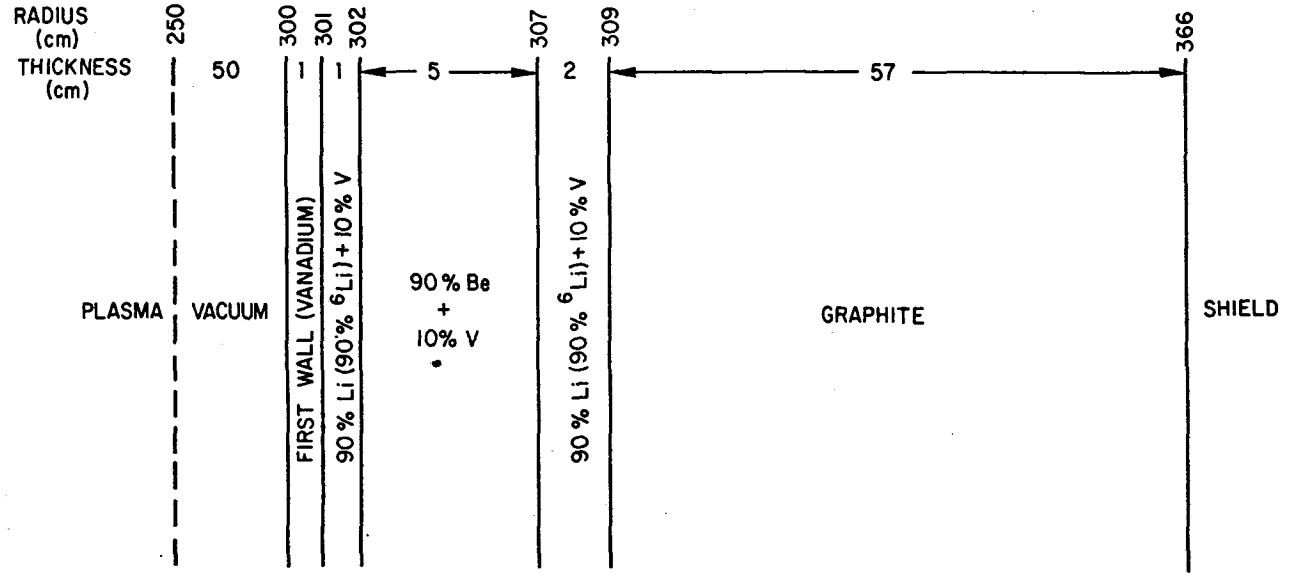

Fig. 2. A schematic of a blanket design with low lithium inventory (design 4).

TABLE IV

Summary of the Neutronics Results for the Designs Described in Table III

Design Number	1	2	3	4	5	6	7	8	9	10
$^6Li(n,\alpha)t$	0.928	1.469	1.370	1.150	1.159	1.077	1.183	0.979	1.093	0.988
$^7Li(n,n'\alpha)t$	0.001	0.004	0.005	0.006	0.035	0.003	0.010	0.002	0.003	0.003
Tritium breeding ratio	0.929	1.473	1.375	1.156	1.194	1.080	1.193	0.981	1.096	0.991
Neutron heating[a]	13.71	15.82	14.94	13.46	13.49	12.74	13.67	11.89	12.85	
Gamma heating	7.97	3.74	2.68	2.31	2.37	2.94	2.30	3.82		
Total heating	21.68	19.56	17.62	15.77	15.86	15.68	15.97	15.71		
Neutron leakage[a]	0.03	0.03	0.06	0.09	0.08	0.07	0.07	0.04	0.08	0.07
$Be(n,2n)$[b]	1.002	0.947	0.746	0.505	0.491	0.469	0.468	0.364	0.485	0.423
$(n,2n)$[c] in V or SS	0.124	0.128	0.124	0.118	0.122	0.115	0.114	0.118	0.117	0.069
(n,γ)[c] in V or SS	0.629	0.195	0.072	0.021	0.023	0.033	0.014	0.068	0.030	0.026

[a]In units of MeV per DT neutron.
[b]All reactions are given in units of reactions per DT neutron.
[c]Vanadium in designs 1 through 9 and stainless steel in design 10.

The results in Table IV for designs 4, 6, 7, and 9 compare the neutronics performance of lithium, $Li_2Al_2O_4$, Li_2O, and LiAl as breeding materials. Since the comparison is on the basis of equal volumes of each compound, the amount of lithium varies greatly from design to design as can be seen from comparing the number of lithium atoms per unit volume in these compounds as given in Table II. The tritium production in these compounds is affected mainly by two factors: (a) the lithium nuclide number density per unit volume in the compound, and (b) the presence of such other elements as oxygen and aluminum. The first factor simply means that the larger the lithium optical thickness, the larger the tritium breeding ratio. However, for the same amount of beryllium, the increase in the tritium breeding ratio, as the lithium concentration is increased beyond 2×10^{22} atom/cm^3 in the 3-cm lithium compound layer, is modest, since this amount of highly enriched lithium already represents several mean-free-paths for tritium production. The presence of oxygen and aluminum, on the other hand, has two opposite effects on the breeding ratio. Some of the high-energy neutrons streaming into the breeding zones are slowed down by inelastic scattering. This prevents most of these neutrons from having a chance of inducing an $(n,2n)$ reaction if they stream back into the beryllium region, thus reducing the blanket neutron multiplication. However, these neutrons as they are slowed down will have a greater probability of inducing a $^6Li(n,\alpha)t$ reaction. In addition, the presence of oxygen and aluminum results in some parasitic capture. Nevertheless, the optical thickness of oxygen and aluminum in any of the compounds considered in the designs presented here is only a small fraction of a mean-free-path for collision by high-energy neutrons. All the factors considered above that have opposite effects on the breeding ratio cause the variation of the ratio to be rather small from one compound to another. Note that since the variation in the lithium concentration is very large (it varies by a factor as large as 4, see Table II) the tritium breeding ratio is higher for the compounds with higher lithium nuclide number density.

Inspection of the results for designs 4 and 5 show that varying the enrichment of lithium in ^6Li while keeping the optical thickness of ^6Li the same does not significantly change the neutronics characteristics of the system. If the lithium enrichment and thickness are varied, however, such that the optical thickness of ^7Li is close to one average mean-free-path or more, the change in the results is more pronounced.

Although metallic beryllium is less favorable from a materials point of view than beryllium oxide or beryllium carbide, it is desirable from a neutronics standpoint not to introduce any elements other than beryllium into the neutron multiplication regions in the blanket. Neutron interactions in such elements compete with the $(n,2n)$ reaction in beryllium decreasing the efficiency of beryllium utilization. Design 8, which utilizes BeO, produces a breeding ratio ~8% smaller than that of design 6, which employs metallic beryllium, although the amount of beryllium in the former is slightly larger than that in the latter. Thus the amount of beryllium required per blanket is larger when beryllium compounds are used. This is undesirable if beryllium resources are as limited as present studies indicate. Note, however, that beryllium burnup is

approximately the same in beryllium and beryllium compounds for the same neutron multiplication. Another disadvantage of using beryllium compounds, although not of great importance in this case, is the associated increase in the physical thickness of the blanket.

Designs 1 through 9 utilize vanadium as first wall and structure. Design 10, however, is the same as that of design 6 except for replacing vanadium with stainless steel on an equal volume basis. Although the (n,γ) reaction rate in vanadium is greater than in stainless steel, the breeding ratio is smaller in design 10 than in design 6. Stainless steel is more effective than vanadium in slowing down the high-energy neutrons and, therefore, it reduces the rate of neutron multiplication in beryllium. In addition, the $(n,2n)$ reaction rate in vanadium is larger than that in stainless steel.

In designs 4 through 10, the tritium breeding required is achieved by ~3 cm of highly enriched lithium and 5 cm of beryllium plus structure in addition to a 1-cm first wall. The average energy carried away with the neutrons leaking out of zone 8 in these designs (see Table III) is 3 to 4 MeV per DT neutron. Therefore, an additional region is required beyond the neutron multiplication and tritium production zones to (a) extract the kinetic energy remaining with the neutrons, and (b) moderate and reflect a fraction of the neutrons into the tritium breeding zones, thus increasing the tritium production density that in turn allows reduction of the lithium inventory and/or the amount of beryllium required. We employed graphite to perform these functions in all designs (see zone 9 in Table III). Some of the alternatives were eliminated on the basis of material performance. Some others were excluded on the basis of their undesirable neutronics characteristics. For example, the strong neutron absorption in boron prevents adequate tritium breeding with reasonable beryllium inventories if boron carbide (B_4C) is used instead of graphite. Similarly, the parasitic capture in stainless-steel constituents reduces significantly the tritium breeding ratio when it is used in zone 9. Although graphite has several disadvantages[50] regarding its behavior under irradiation, it seemed a reasonable choice for the type of designs considered in this study.

Note that an additional zone of ~1 cm of highly enriched lithium behind the graphite can increase the tritium production significantly, thus increasing the breeding ratio or allowing a smaller amount of beryllium to be used. This has two disadvantages, however. First, segmenting the tritium breeding region into several zones can complicate the tritium extraction system. Another disadvantage is related to the high lithium burnup in the designs considered here, as will be discussed later, requiring replacement of the breeding zones every few years depending on the magnitude of the wall loading. Thus, an additional breeding zone outside the bulky graphite region makes the replacement schemes more difficult.

IV. THE UWMAK-II DESIGN

The foregoing considerations were the basis for the blanket and shield design of the second 5000-MW(th) University of Wisconsin Tokamak Conceptual Reactor,[51] called UWMAK-II. In this section, we present the results of the neutronics and tritium extraction and removal studies.

A schematic of the UWMAK-II blanket and shield is given in Fig. 3. While the reactor is toroidal in geometry, with a minor plasma radius of 5 m and a major radius of 13 m, the neutron and gamma-ray transport calculations were carried out in cylindrical geometry using the same calculational techniques described in the previous section. Based on the discussion given in Sec. II and on such other considerations as fabricability and the presence of qualified technology, stainless steel is chosen as the material for the first wall, structural components, and helium-coolant tubing. The first-wall thickness was determined from considerations that included hoop and thermal stresses, sputtering, blistering, and corrosion problems. The physical thickness of the first wall is 2 cm, but 50% of the volume is occupied by the helium coolant. Since helium does not perturb the transport calculations to any measurable degree, a density factor of 0.5 for stainless steel in the 2-cm wall was used (see Fig. 3).

The stainless steel required for the structural components and coolant tubing was estimated as 10% of the physical volume of the blanket and shield. The blanket is conceived as composed of cells, each 20 cm wide and 90 cm deep; and the stainless-steel cell walls are ~7 mm thick. The lithium aluminate and beryllium will be packed in pins with an average stainless-steel wall of 0.75 mm. Obviously, the neutronics for such a system can best be predicted by three-dimensional calculations. However, for the approximate one-dimensional calculation, the stainless-steel structure must be homogenized with the other blanket and shield constituents. Since most of the neutrons in the beryllium and lithium aluminate regions of the actual system will not suffer any interaction in the stainless-steel structure, a homogenization scheme based on the actual volume percentage of the structure in each zone would overestimate the neutron interaction rate in stainless steel, thus underpredicting the actual

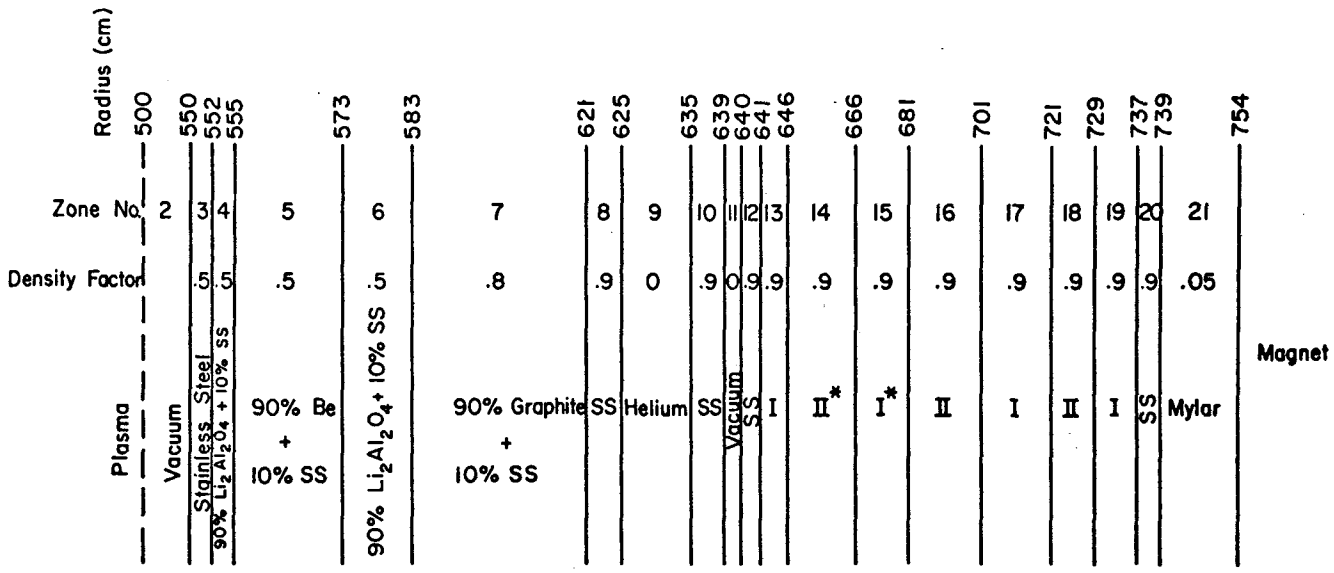

* Material I is a mixture of 90% B_4C and 10% SS and material II is a mixture of 90% Pb + 10% SS.

Fig. 3. A schematic of UWMAK-II blanket and shield.

reaction rates in beryllium and lithium aluminate. At the time, no studies of detailed cells were available, and to compensate for the above effect, we homogenized 50% of the structure in the inner region of the blanket with beryllium and lithium aluminate and placed the rest of the structure in the outer regions (with the stainless steel in zones 8 and 10 of Fig. 3) for the one-dimensional calculations.

Zones 4 and 6 in Fig. 3 are the tritium production zones. They are 3 and 10 cm thick, respectively, and the lithium is enriched to 90% in ^6Li. Lithium aluminate was chosen as the breeding material for the reasons discussed earlier. Due to the slow tritium diffusion predicted (Fig. 1), the lithium aluminate must be fabricated as very small pellets. Thus a large void fraction exists in the lithium aluminate. A 50% packing fraction appears reasonable. Zone 5 is an 18-cm-thick region of 90% beryllium plus 10% stainless steel. A density factor of 0.5 is used in this zone to accommodate the swelling resulting from excessive helium production in the beryllium.

Zone 7 is 38 cm of 90% graphite plus 10% stainless steel. The graphite serves as moderator for the high-energy neutrons streaming out of the neutron multiplication and tritium production zones and reflects some of the neutrons back into these zones. Because of the relatively large helium production rate in graphite, a density factor of 0.8 is used in the graphite zone.

The headers for the primary helium coolant are idealized in the one-dimensional model by zones 8, 9, and 10. The 8 cm of stainless steel in zones 8 and 10 serve also as a neutron reflector, and they extract the greater part of the useful kinetic energy remaining with the neutrons and photons.

Zone 11 is a 1-cm vacuum gap, and it serves as a thermal barrier between the high-temperature blanket (~600°C) and the low-temperature shield (~200°C). Zones 12 through 20 comprise the magnet shield. The shield composition and dimensions resulted from optimizing the total cost of the shield, magnet, and the helium refrigerators required to cool the superconducting magnet to ~4 K, using the optimization technique described in Ref. 52. Excluding zones 12 and 20, the shield is 96 cm and consists of alternating zones of lead and boron carbide on an equal volume basis with 10% of the total volume occupied by stainless steel for structural purposes. The 1 cm of stainless steel in zone 12 is a structural support for the heavy weight of the shield. Zone 20, which is 2 cm of stainless steel, is a part of the magnet, and it represents the dewar for the cryogenic system. Zone 21 is thermal insulation for the magnet and cryogenic systems, and ~95% of this zone is vacuum to prevent heat transfer by conduction. The mylar superinsulation reduces the thermal radiation losses.

We turn our attention now to a discussion of the results for the UWMAK-II reactor just described. The neutronics results in particular are presented in detail as they provide the basic input to other areas of the reactor design.

Neutron heating is given by material and zone in Table V. In Table VI, the neutron and gamma-ray heating and the gamma-ray energy production are tabulated by zone. The results in these tables are given in units of MeV per DT neutron. Several observations are in order. The neutron heating in ^{6}Li alone is one-third of the total nuclear heating in the system, and the average heating rate per unit volume in the first wall is 9.95 W/cm^3 per MW/m^2. The maximum power density in the blanket is in the lithium-aluminate stainless-steel region behind the first wall. The average power density in this region is 17.81 W/cm^3 per MW/m^2 compared with 6.39 in the lithium-

TABLE V

Neutron Heating in UWMAK-II by Material and Zone (in units of MeV per DT neutron)

Zone	Composition	Cr	Ni	Fe	Be	^{6}Li	^{7}Li	O	Al
1	Plasma								
2	Vacuum								
3	Stainless steel	0.0823	0.1293	0.3794					
4	90% $Li_2Al_2O_4$ + 10% SS	0.0095	0.0153	0.0439		2.7297	0.0206	0.3566	0.1988
5	90% Be + 10% SS	0.0290	0.0488	0.1334	3.9784				
6	90% $Li_2Al_2O_4$ + 10% SS	0.0064	0.0110	0.0292		3.4098	0.0171	0.2650	0.1374
7	90% C + 10% SS	0.0104	0.0181	0.0471					
8	Stainless steel	0.0021	0.0034	0.0092					
9	Helium	---	---	---	---	---	---	---	---
10	Stainless steel	0.0012	0.0019	0.0054					
11	Vacuum	---	---	---	---	---	---	---	---
12	Stainless steel	2.25 (-4)[a]	3.46 (-4)	9.80 (-4)					
13	90% B_4C + 10% SS	7.92 (-5)	1.26 (-4)	3.47 (-4)					
14	90% Pb + 10% SS	1.24 (-4)	1.70 (-4)	5.26 (-4)					
15	90% B_4C + 10% SS	1.34 (-5)	1.92 (-5)	5.71 (-5)					
16	90% Pb + 10% SS	2.91 (-6)	3.90 (-6)	1.22 (-5)					
17	90% B_4C + 10% SS	3.21 (-7)	4.57 (-7)	1.36 (-6)					
18	90% Pb + 10% SS	1.69 (-8)	2.64 (-8)	7.29 (-8)					
19	90% B_4C + 10% SS	6.77 (-9)	1.11 (-8)	2.94 (-8)					
20	Stainless steel	8.32 (-9)	1.42 (-8)	3.66 (-8)					
Sum by material		0.1413	0.2285	0.6495	3.9784	6.1395	0.0377	0.6216	0.3362

Zone	C	^{10}B	^{11}B	Pb	Sum by Zone
1					0.0
2					0.0
3					0.5910
4					3.3744
5					4.1896
6					3.8759
7	0.8453				0.9209
8					0.0147
9					0.0
10					0.0085
11	---	---	---	---	0.0
12	---	---	---	---	1.551 (-3)
13	2.92 (-3)	9.92 (-2)	8.76 (-3)	---	1.114 (-1)
14	---	---	---	8.55 (-4)	1.675 (-3)
15	5.89 (-4)	1.61 (-2)	1.86 (-3)	---	1.864 (-2)
16	---	---	---	2.18 (-5)	4.081 (-5)
17	1.48 (-5)	4.30 (-4)	4.78 (-5)	---	4.947 (-4)
18	---	---	---	1.14 (-7)	2.30 (-7)
19	2.73 (-7)	5.09 (-6)	8.49 (-7)	---	6.26 (-6)
20	---	---	---	---	5.91 (-8)
Sum by material	0.8488	0.1157	0.0107	0.0009	13.109

[a] 2.25×10^{-4}.

TABLE VI

Neutron and Gamma-Ray Heating, Gamma-Ray Energy Production, and Total Heating in UWMAK-II by Zone (in units of MeV per DT neutron)

Zone	Thickness (cm)	Density Factor	Composition	Neutron Heating	Gamma-Ray Heating	Gamma-Ray Energy Production	Total Heating
1	500	0.0	Plasma	0.0	0.0	0.0	0.0
2	50	0.0	Vacuum	0.0	0.0	0.0	0.0
3	2	0.5	Stainless steel	0.5910	0.8116	1.1858	1.4026
4	3	0.5	90% $Li_2Al_2O_4$ + 10% SS	3.3744	0.3908	0.6881	3.7652
5	18	0.5	90% Be + 10% SS	4.1896	1.2492	1.0289	5.4388
6	10	0.5	90% $Li_2Al_2O_4$ + 10% SS	3.8759	0.6289	0.5535	4.5048
7	38	0.8	90% C + 10% SS	0.9209	1.3990	1.1453	2.3199
8	4	0.9	Stainless steel	0.0147	0.2695	0.2394	0.2842
9	10	0.0	Helium	~0.0	~0.0	~0.0	~0.0
10	4	0.9	Stainless steel	0.0085	0.1263	0.0861	0.1348
11	1	0.0	Vacuum	0.0	0.0	0.0	0.0
12	1	0.9	Stainless steel	1.551 (-3)[a]	1.74 (-2)	1.04 (-2)	1.895 (-2)
13	5	0.9	90% B_4C + 10% SS	1.114 (-1)	1.89 (-2)	4.55 (-3)	1.303 (-1)
14	20	0.9	90% Pb + 10% SS	1.675 (-3)	4.57 (-2)	1.32 (-2)	4.738 (-2)
15	15	0.9	90% B_4C + 10% SS	1.864 (-2)	5.51 (-4)	7.00 (-4)	1.915 (-2)
16	20	0.9	90% Pb + 10% SS	4.081 (-5)	4.47 (-4)	3.2 (-4)	4.878 (-4)
17	20	0.9	90% B_4C + 10% SS	4.947 (-4)	1.47 (-5)	1.75 (-5)	5.097 (-4)
18	8	0.9	90% Pb + 10% SS	2.30 (-7)	4.48 (-6)	2.21 (-6)	4.710 (-6)
19	8	0.9	90% B_4C + 10% SS	6.26 (-6)	3.73 (-7)	4.45 (-7)	6.633 (-6)
20	2	0.9	Stainless steel	5.91 (-8)	2.44 (-7)	3.01 (-7)	3.031 (-7)
Sum (in MeV per DT neutron)				13.109	4.958	4.958	18.067

[a]To be read as 1.551×10^{-3}.

aluminate stainless-steel mixture in zone 6 and 4.29 W/cm^3 per MW/m^2 in the beryllium stainless-steel zone. The nuclear heating in the shield is only 1.2% of the total nuclear heating in the blanket and shield, i.e., ~50 MW for the 5000-MW(th) reactor. Thus, extracting this amount of energy at high efficiency is not necessary, but its removal is crucial to ensure the physical integrity of the lead containing shield.

A summary of the results for the tritium breeding, nuclear heating, energy leakage from the magnet shield, and radiation damage parameters in UWMAK-II is given in Table VII. For purposes of comparison, we listed in this table the same parameters for the University of Wisconsin First Conceptual Reactor Design,[1] UWMAK-I. The UWMAK-I blanket consists of a 0.4-cm stainless-steel first wall, 56 cm of 90% natural lithium plus 10% stainless steel, and a 17-cm stainless-steel reflector. The major differences between UWMAK-I and the UWMAK-II blanket presented here is the lithium inventory, which is 1.4×10^6 kg in UWMAK-I, while only 4.1×10^4 kg in UWMAK-II. This also results in a much lower tritium inventory as discussed later in this section.

Table VII shows that the contribution of ^{7}Li to tritium production is very small and that the tritium breeding ratio of 1.18 comes almost entirely from the ^{6}Li$(n,\alpha)t$ reaction. This is in contrast to reactors operating on a high-energy spectrum in natural lithium, in which ~40% of the tritium breeding comes from the ^{7}Li$(n,n'\alpha)t$ reaction, as shown for UWMAK-I in Table VII. It is important to note that 0.01 tritium atoms per DT neutron are produced in the Be(n,t) reaction (see Table VIII). While this amount of tritium is not crucial from a breeding point of view, it is extremely important to extract it as it represents a production rate of ~6 g/day in a 5000-MW(th) reactor, and allowing it to accumulate in the beryllium would increase the tritium inventory in the blanket significantly.

The total energy deposition in the blanket and shield of the UWMAK-II design is shown in Table VII to be ~18 MeV, which is 1.5 MeV higher than that in the UWMAK-I. This can be explained on the basis of the additional $(n,2n)$ reactions in beryllium and the increase in the exothermic reactions in the highly enriched lithium in the UWMAK-II.

Note from Table VII that the nuclear radiation load to the magnet in UWMAK-II is only 256 W, which is more than an order of magnitude lower than that in UWMAK-I. The reasons for the

TABLE VII

Summary of Tritium Breeding, Nuclear Heating, Energy Leakage, and Radiation Damage Parameters in the UWMAK-II Design

(Results for UWMAK-I are shown for comparison.)

Parameter	UWMAK-II	UWMAK-I
$^6Li(n,\alpha)t$	1.1801	0.8835
$^7Li(n,n'\alpha)t$	0.0034	0.6037
Tritium breeding ratio	1.1835	1.4872
Neutron heating	13.1088	12.43
Gamma-ray heating	4.9563	4.13
Total heating (in units of MeV/DT neutron)	18.0651	16.56
Neutron energy leakage to the magnet	0.844×10^{-6}	1.5×10^{-5}
Gamma-ray energy leakage to the magnet (in units of MeV/DT neutron)	0.137×10^{-6}	0.321×10^{-6}
Total nuclear radiation load to the magnets (W)	256	3840
In Stainless-Steel First Wall		
Atomic displacements (dpa/yr per MW/m^2)	10.3	11.0
Helium production (ppm/yr per MW/m^2)	200	219
Hydrogen production (ppm/yr per MW/m^2)	525	595

better attenuation in the UWMAK-II shield are as follows. The cost optimization for UWMAK-II is based on a price of 3$/kg for B_4C, while 15$/kg was assumed in UWMAK-I calculations. The lower price was used as it appears to be more realistic at present. Thus, the optimum shield[52] of UWMAK-II is 96 cm of 50% lead plus 50% B_4C, in contrast to 75 cm of 70% lead plus 30% B_4C in UWMAK-I. The 50% lead plus 50% B_4C mixture is more efficient in total energy attenuation than the 70% lead plus 30% B_4C mixture.

Parameters of interest in radiation damage analysis to the stainless-steel first wall are given in Table VII. The atomic displacement rate is ~10 dpa/yr per MW/m^2. The helium and hydrogen production rates are 200 and 525 ppm/yr per MW/m^2, respectively. These rates (and the rates of other high-energy reactions in general) are ~10% lower than those in UWMAK-I because the beryllium and lithium aluminate behind the first wall are more effective in slowing down the neutrons than the natural lithium employed in UWMAK-I. The implications of these high displacement and gas production rates from a radiation damage standpoint are as serious as those in UWMAK-I (Ref. 1). For the design value of 1.16 MW/m^2 neutron wall loading, the wall life is still limited to <2 yr by loss of ductility.

The question of lithium burnup in the UWMAK-II design is important. From the neutronics results discussed above, ^6Li is burned at a rate of 1.34%/yr per MW/m^2. The lithium inventory is 4.1×10^4 kg of lithium enriched to 90% in ^6Li. Thus, 5.6×10^5 kg of natural lithium would be enriched to supply the initial loading of the UWMAK-II reactor. The 480 kg of ^6Li consumed per year per MW/m^2 would come from 7500 kg of natural lithium. It is of interest to compare the lithium utilization in this system with other designs employing natural lithium such as UWMAK-I. The percentage burnup rate of ^6Li in UWMAK-I is nearly 19 times that of ^7Li. Thus, in terms of resources, ^6Li consumption is the crucial factor as in UWMAK-II although the efficiency of lithium resources utilization is different. If the UWMAK-I blanket is redesigned to produce the same breeding ratio as UWMAK-II, the rate of the $^6Li(n,\alpha)t$ reaction would be ~0.7 reactions per DT neutron compared with 1.18 in UWMAK-II. Hence the rate of consumption of ^6Li in UWMAK-II is ~70% larger than in UWMAK-I. In addition to the relatively inefficient utilization of lithium resources in UWMAK-II type of reactors, the large amounts of ^7Li generated from lithium enrichment is a potential problem. One way to alleviate this problem is to employ some of this ^7Li as reflector-moderator instead of graphite in the reactor. However, tritium will inevitably be produced in ^7Li, resulting in a large tritium inventory in the blanket; this would negate the principal purpose for building the UWMAK-II type of reactor.

Note also that ^6Li burnup in the UWMAK-II

blanket is not uniform; it varies significantly from one position to another. The average ^{6}Li burnup rate is 2.5 and 1%/yr per MW/m^2 in zones 4 and 6, respectively. A maximum burnup rate of 7.8%/yr per MW/m^2 occurs in the portion of zone 4 adjacent to the beryllium region (see Fig. 3). The drop in the tritium breeding ratio in the first year of operation at a 1 MW/m^2 neutron wall loading was estimated to be 1.7%. This suggests that a ^{6}Li makeup is required every few years if the breeding ratio is to be kept above one. In addition, the chemical change and the heat generation rates in the lithium aluminate will be very large at those positions where the lithium burnup is highest. The use of a high melting compound such as lithium aluminate is a necessity at these positions.

A summary of other results of importance are given in Table VIII. The $(n,2n)2\alpha$ and (n,α) reaction rates in beryllium are 0.59 and 0.05 reactions per DT neutron. Thus ~8 cm^3 of helium (STP) are generated per cm^3 of beryllium per year for a neutron wall loading of 1 MW/m^2. Further studies are required to analyze the swelling problem in beryllium under such an excessive helium production rate. As indicated earlier, the tritium production rate in beryllium is significant, 0.01 tritium atoms per DT neutron, and some means for tritium removal from the beryllium region must be provided.

TABLE VIII

Summary of Results for Some Nuclear Reactions of Interest in UMAK-II

Parameter	UWMAK-II
Reaction Rates in Beryllium	
(in units of reactions/DT neutron)	
$(n,2n)$ 2α	0.5928
(n,γ)	0.0024
(n,p)	3.97×10^{-5}
(n,t)	0.0105
(n,α)	0.0532
Average helium production rate in beryllium (in units of ppm/yr per MW/m^2)	1730
Maximum helium production rate in graphite (in units of ppm/yr per MW/m^2)	193
Average helium production rate in boron	12.9
Average tritium production rate in boron (in units of ppm/yr per MW/m^2)	0.03
(n,γ) Reaction Rate (reactions/DT neutron)	
Chromium	0.0337
Nickel	0.0284
Iron	0.1081
Aluminum	0.0017
Oxygen	4.0×10^{-6}
^{6}Li	5.2×10^{-5}
^{7}Li	5.0×10^{-6}
Beryllium	0.0024
Graphite	0.0007
Sum over (n,γ) reaction in the blanket	0.1751

It can be seen from Table VIII that ~0.66 beryllium atoms are burned per DT neutron. Thus the burnup rate for beryllium is 0.09%/yr per MW/m^2. This rate has a small effect on the neutronics behaviors of the blanket for a plant operation of 30 yr. The beryllium inventory in UWMAK-II (see Fig. 3) is 4.33×10^5 kg. Thus 1.17×10^4 kg of beryllium are burned in UWMAK-II if the reactor is operated for 30 yr with a neutron wall loading of 1 MW/m^2. This again raises the question of the availability of beryllium resources, which needs to be studied in detail.

The tritium inventory in the blanket of UWMAK-II and its potential leakage into the steam cycle have been estimated and summarized in Table IX, based on the breeding material selected and the blanket design shown in Fig. 3. The decision to utilize the ceramic compound, $LiAlO_2$, as the tritium breeding material was made because of its good high-temperature properties, as compared to the other lithium compounds discussed in Sec. II. Additionally, the design criterion was to prevent, if possible, the contamination of the helium coolant by fine particles of the tritium breeding materials. To accomplish this objective, the blanket of the reactor would be composed of stainless-steel modules nearly 90 cm thick. Helium at a pressure of 50 atm would enter each module so that the first wall would be cooled initially, followed by the cooling of the beryllium, $LiAlO_2$, and graphite zones. The temperature of the first wall would be maintained below 585°C, while the helium temperature would approach 650°C on exit from the module.

Inside of each large blanket module, the beryllium and $LiAlO_2$ would be contained in stainless-steel pins ~3.5 cm in diameter, nearly 30 cm long, and with a wall thickness of 0.75 mm. These tubes would be closed at one end, with the other end attached to a small gas plenum, connected to a tritium extraction system external to the reactor. The beryllium was placed in the same tubes as the $LiAlO_2$ so that the tritium from both materials would be extracted simultaneously. The tritium pressure inside the tubes would be maintained at 10^{-4} Torr either by evacuation or by the circulation of helium through these tubes. The graphite would be encased in separate stainless-steel cans, nearly 40 cm long, and placed behind the breeding material.

Because of the low thermal conductivity predicted for $LiAlO_2$, a centerline temperature of >1300°C is estimated for this material in the

TABLE IX

Tritium Breeding and Recovery

	UWMAK	
	II	I
Coolant	helium (10^6 moles)	lithium (2×10^8 moles)
T_2 breeder	$^6LiAlO_2$	lithium
Li in blanket, kg	4.1×10^4	1.4×10^6
Coolant temperature, maximum (°C)	650	483
Tritium Inventory in Breeder		
Solubility	7.0 g	8.7 kg
Diffusion, 10-μm path	33.0 g	0
Total	40.0 g	8.7 kg
Tritium pressure in breeding zone (Torr)	10^{-4}	5.0×10^{-10}
Tritium pressure for diffusion into steam (Torr)	1.6×10^{-14}	3.8×10^{-11}
Tritium generation rate, g/sec	1×10^{-2}	1.22×10^{-2}
Additive to coolant	O_2 (10^{-2} Torr)	none
Tritium species in coolant for recovery	T_2O	T(Li)
Extraction bed	Molecular Sieves	Yttrium Metal
τ (coolant transit time), sec	1	254
Fraction coolant to bed	0.7%	4%
Intermediate heat exchange	none	sodium
Tritium leakage to steam, Ci/day	1.0	10
Heat exchanger, coolant-steam	SS	SS
Area, cm^2	8.3×10^8	3.2×10^8
Thickness, mm	4.0	1.65
Temperature, average, °C	460	296

stainless-steel pins, while the surface temperature is ~600°C. An average fuel temperature of 900°C is assumed, therefore, to estimate the diffusion and solubility of tritium in this ceramic compound. At this temperature, the predicted diffusion coefficient, Fig. 1, is $\sim 10^{-10}$ cm^2/sec, with an uncertainty of about an order of magnitude. Consequently, particles in which the maximum tritium path lengths for migration are ~10 μm are required to maintain the tritium inventory below 100 g as discussed in Sec. II. This requirement can be met either by the utilization of crushed powder ~20 μm in diameter or by the fabrication of porous ceramic bodies with a nominal 20 μm between pores. By the use of such small particles, the tritium retention due to diffusion is ~33 g for the total reactor.

The solubility of tritium in $LiAlO_2$, estimated from the hydrogen solubility in zinc oxide, as discussed in Sec. II, is ~0.3 $cm^3/(cm^3\ atm^{1/2})$; consequently, at a tritium pressure of 10^{-4} Torr, the solubility of the tritium in the $LiAlO_2$ is ~7 g. Therefore, the steady-state inventory of tritium in the ceramic breeder is only 40 g. The largest uncertainty in these estimates is associated with the diffusion coefficient for tritium in $LiAlO_2$; consequently, the tritium inventory in the ceramic breeder can have an uncertainty of about an order of magnitude. By comparison, the tritium solubilities in the beryllium and stainless steel in the breeder pins are small, <2 and 6 g, respectively.

A significant amount of tritium will diffuse through the pins containing the breeder material and contaminate the helium coolant because of the large surface area of the pins, nearly 3.3×10^8 cm^2. A steady-state condition will be attained in which the amount of tritium permeating into the helium system will equal the amount that permeates out of the system through the steam generator. At this steady-state condition, the tritium pressure in the helium will approach 9.94×10^{-5} Torr, and nearly 3.6 g/day (3.6×10^4 Ci/day) of tritium would permeate into the steam system and be transferred eventually to the environment.

Previous studies[2] have shown that the loss of tritium through the heat transfer system represents the most significant routine pathway for

tritium escape from a fusion power plant. To prevent a large loss of tritium through this pathway, a scheme is suggested for tritium removal from the helium that is compatible with the presently proposed blanket design. In this scheme, oxygen at partial pressure of 10^{-2} Torr is maintained in the helium so that the following equilibrium is established

$$T_2 + \tfrac{1}{2}O_2 = T_2O \ .$$

A catalyst may be required in the helium circuit to establish this equilibrium rapidly. The equilibrium constant[53] for this reaction at 525°C, the median temperature in the helium blanket, is $\sim 6 \times 10^{11}$ Torr$^{-1/2}$; consequently, if the partial pressure of T_2O is maintained below 10^{-3} Torr, then the partial pressure of tritium (T_2) is only 2×10^{-14} Torr. At this low tritium partial pressure, only ~1.0 Ci/day of tritium permeates into the steam system. This permeation might be reduced further if a diffusion barrier is developed for use in the helium-steam heat exchanger.

The continuous absorption of T_2O on molecular sieves is proposed to maintain the T_2O vapor pressure below 10^{-3} Torr. Such an absorption bed[54] operating at 95°C has an equilibrium vapor pressure of 5×10^{-4} Torr (water) when it has absorbed 0.5 g of water per 100 g of absorbant. If the vapor pressure of T_2O on this dessicant is similar to that of water, and if the bed is recycled whenever the vapor pressure of T_2O exceeds 5×10^{-4} Torr, then only 0.7% of the helium per cycle must transit the absorption bed, based upon the tentative cooling system design in which the total helium (10^6 g-mole) flows through the complete circuit in 1 sec.

Nearly 48 g/day of tritium diffuses into the helium coolant forming 8 g-mole of T_2O. Based on the bulk density of 640 kg/m^3 of molecular sieves, an absorption bed requiring only 0.044 m^3 of molecular sieves is sufficient to absorb one day's generation of T_2O in the helium.

The tritium inventory in the plasma region of a fusion reactor depends mainly on the plasma characteristics and reactor power performance. It does not depend on the scheme for tritium removal from the blanket. However, the amount of tritium on the plasma side at any given time is on the order of a few grams, which is much less than the tritium inventory in the primary energy conversion system.

V. SUMMARY AND CONCLUSIONS

A CTR blanket design that minimizes both lithium and tritium inventories was investigated. The lithium inventory is minimized by employing a thin layer of ^{6}Li operating in soft neutron spectrum obtained by slowing down the DT neutrons in a beryllium compound. Tritium inventory is lowered by increasing the tritium production per unit volume of the breeder in addition to utilizing an efficient tritium extraction system. Lithium was excluded as a coolant and moderator and other candidates were examined.

The survey of the physical properties and predicted irradiation behavior of several lithium bearing materials indicates that $LiAlO_2$ is preferred for a fusion reactor breeder blanket. It is amenable to large-scale fabrication, useful in the 1300 to 1400°C temperature range, and compatible with stainless steel and other blanket materials. Its undesirable characteristics are its low thermal conductivity, its low lithium atom density, and its introduction of neutronically undesirable atoms into the breeding zone.

BeO and Be_2C are more compatible with the structural materials and have better resistance to radiation damage than metallic beryllium. However, the presence of oxygen or carbon in the neutron multiplication zone has detrimental effects on the efficiency of beryllium utilization. The neutronics characteristics of the blanket were found to be very sensitive to the amount of beryllium and the configuration of the breeding and neutron multiplication zones. A 5-cm-thick region of beryllium is a minimum for achieving a tritium breeding ratio of 1.15.

A detailed description of a complete blanket and shield design of a conceptual fusion reactor, UWMAK-II, based on the considerations of this study, was presented. The blanket uses stainless steel for the first wall and structure, lithium aluminate enriched to 90% ^{6}Li for tritium breeding, metallic beryllium for neutron multiplication and moderation, and graphite for additional neutron moderation. The blanket is helium cooled.

The tritium breeding ratio in the present study of UWMAK-II is 1.18, and the total nuclear heating is 18 MeV per DT neutron. The lithium inventory is only 4.1×10^4 kg compared with 1.4×10^6 kg in the earlier UWMAK-I (Ref. 1), which employs natural lithium for breeding, neutron moderation, and cooling.

The power density in the breeding zones is high with a maximum of nearly 20 W/cm^3 per MW/m^2. The diffusion coefficient with an average temperature of 900°C in the lithium aluminate limits the tritium path to ~10 μm to keep the tritium inventory below 100 g. The tritium produced in beryllium at a rate of 0.01 tritons per DT neutron requires a provision for removal. Thus the beryllium is contained with the lithium aluminate particles in stainless-steel pins that are attached at one end to a gas plenum connected to the

tritium extraction system. The tritium pressure inside the pins is maintained at 10^{-4} Torr. Each pin is cooled externally with helium at 50 atm. The steady-state inventory of tritium in the ceramic is estimated to be only 40 g, which is a factor of ~250 lower than in UWMAK-I.

A scheme for tritium removal from the primary helium coolant, based on the oxidation of tritium to form tritiated water absorbed on a molecular sieve dessicant, was found to be successful in keeping the tritium leakage to the steam to ~1 Ci/day.

The maximum and average burnup rates of ^{6}Li were calculated as 7.8 and 1.34%/yr per MW/m^2. Depending on the operating conditions, the breeding material may need to be replaced every few years. The effects of the excessive helium production rates in the solid breeder and the beryllium metal need to be studied in more detail.

In conclusion, if appears feasible to design a CTR blanket with low lithium and tritium inventories in a solid breeding material. These blankets offer several advantages from plant reliability and safety standpoints.

REFERENCES

1. B. BADGER et al., "UWMAK-I, A Wisconsin Toroidal Fusion Reactor Design," UWFDM-68, University of Wisconsin (1974).

2. T. A. COULTAS, J. E. DRALEY, V. A. MARONI, and R. A. KRAKOWSKI, "An Environmental Impact Study of a Reference Theta-Pinch Reactor (RTPR)," *Proc. 1st Topl. Mtg. Technology of Controlled Nuclear Fusion,* CONF-740402, U.S. Atomic Energy Commission (1974).

3. M. A. ABDOU and C. W. MAYNARD, "Neutronics and Photonics Study of Fusion Reactor Blankets," *Proc. 1st Topl. Mtg. Technology of Controlled Nuclear Fusion,* Vol. II, CONF-740402, U.S. Atomic Energy Commission (1974).

4. J. DARVAS, "A Design with Low Lithium and Tritium Inventories," presented at the IAEA Workshop on Fusion Reactor Design, International Atomic Energy Agency, Culham (1974).

5. DAI-KAI SZE, University of Wisconsin, Private Communication (1974).

6. Y. SEKI, K. SAKO, K. TANAKA, and T. HIRAOKO, "Tritium Breeding in Ceramic Lithium-Compound Blanket," *Proc. 1st Topl. Mtg. Technology of Controlled Nuclear Fusion,* CONF-740402, U.S. Atomic Energy Commission (1974).

7. J. POWELL, A. ARONSON, P. BEZLER, F. MILES, and W. WINSCHE, "Minimum Activity Blankets Using Aluminum Structure," *Proc. 1st Topl. Mtg. Technology of Controlled Nuclear Fusion,* CONF-740402, U.S. Atomic Energy Commission (1974).

8. D. K. SZE and W. E. STEWART, "Use of Electrical Insulation in Lithium-Cooled Fusion Reactor Blankets," *Proc. 1st Topl. Mtg. Technology of Controlled Nuclear Fusion,* CONF-740402, U.S. Atomic Energy Commission (1974).

9. *Chemical and Engineering News,* p. 14 (June 3, 1974).

10. B. R. T. FROST, "Refractory Metals—Alloys and Properties," *Fusion Reactor First-Wall Materials,* WASH-1206, U.S. Atomic Energy Commission (1972).

11. J. H. DEVAN, "Compatibility," *Fusion Reactor First-Wall Materials,* WASH-1206, U.S. Atomic Energy Commission (1972).

12. M. HANSEN, *Constitution of Binary Atoms,* McGraw-Hill Publishing Co., New York (1958).

13. R. HULTGREN, R. L. ORR, P. D. ANDERSON, and K. K. KELLEY, *Selected Values of Thermodynamic Properties of Metals and Alloys,* p. 48, John Wiley & Sons, Inc., New York (1963).

14. *Handbook of Chemistry and Physics,* 46th ed., Chemical Rubber Co., Cleveland (1964).

15. *Data on Chemicals for Ceramic Use,* Bulletin No. 118, National Research Council, Washington, D.C. (1949).

16. T. YA KOSOLAPOVA, *Carbides,* Plenum Press, New York (1971).

17. J. R. WEIR, "The Effect of High Temperature Reactor Irradiation on Some Physical and Mechanical Properties of Beryllium," *The Metallurgy of Beryllium,* pp. 395-409, Chapman and Hall, London (1963).

18. Y. CARTERET, J. BAREAU, and J. ELSTON, *Brit. Ceramic Soc. Proc.,* **7**, 363 (1967).

19. B. S. HICKMAN and D. G. WALKER, *Brit. Ceramic Soc. Proc.,* **7**, 381 (1967).

20. W. M. MUELLER, J. P. BLACKLEDGE, and G. G. LIBOWITZ, *Metal Hybrides,* pp. 550-551, Academic Press, New York (1968).

21. P. M. S. JONES and R. GIBSON, *J. Nucl. Mater.,* **21**, 353 (1967).

22. K. T. SCOTT and L. L. WASSELL, *Brit. Ceramic Soc. Proc.,* **7**, 375 (1967).

23. K. A. GSCHNEIDNER, Jr., N. KIPPENHAN, and O. D. McMASTERS, "Thermochemistry of the Rare Earths," IS-R1C-6, Iowa State University (1973).

24. W. VICKERS, "The Compatibility of Beryllium with Various Reactor Materials," *The Metallurgy of Beryllium,* pp. 335-349, Chapman and Hall, London (1963).

25. V. A. MARONI, E. J. CAIRNS, and F. A. CAFASSO, "A Review of the Chemical, Physical and Thermal Properties of Lithium that Are Related to Its Use in Fusion Reactors," ANL-8001, Argonne National Laboratory (1973).

26. T. KIKUCHI, Japan Atomic Energy Research Institute, Memo 5837 (1974).

27. D. W. STRICKLER and RUSTUM ROY, *J. Am. Ceramic Soc.*, **44**, 225 (1961).

28. F. C. KRACEK, *J. Phys. Chem.*, **34**, 2641 (1930).

29. W. A. HART and O. F. BEUMEL, Jr., *Comprehensive Inorganic Chemistry*, Vol. I, A. F. TROUTMAN-DICKENSON, Ed., pp. 340-361, Pergamon Press, Oxford (1973).

30. J. S. WATSON, "A Evaluation of Methods for Recovering Tritium from the Blankets or Coolant Systems of Fusion Reactors," ORNL-TM-3794, Oak Ridge National Laboratory (1972).

31. E. RYSHKOWITCH, *Oxide Ceramics*, p. 68, Academic Press, New York (1961).

32. E. GREENSPAN and W. G. PRICE, Jr., "Tritium Breeding Potential of the Princeton Reference Fusion Power Plant," *Proc. 1st Topl. Mtg. Technology of Controlled Nuclear Fusion*, CONF-740402, U.S. Atomic Energy Commission (1974).

33. W. JOST, *Diffusion in Solids, Liquids and Gases*, p. 60, Academic Press, New York (1960).

34. E. W. ROBERTS and J. P. ROBERTS, *Bull. Soc. Franc. Ceram.*, **77**, 3 (1967).

35. V. K. HAUFFE and O. HOEFFGREN, *Ber. Bunsen-Ges. Phys. Chem.*, **74**, 537 (1970).

36. T. S. ELLMAN and K. VERGHESE, *J. Nucl. Mater.*, **53**, 299 (1974).

37. R. G. HICKMAN, "Some Problems Associated with Tritium in Fusion Reactors," *Proc. Technology Controlled Thermonuclear Fusion and Engineering Aspects of Fusion Reactors*, CONF-721111, U.S. Atomic Energy Commission (1974).

38. D. G. THOMAS and J. J. LANDER, *J. Chem. Phys.*, **25**, 1136 (1956).

39. M. STEVANOVIC and J. ELSTON, *Brit. Ceramic Soc. Proc.*, **7**, 423 (1967).

40. R. M. BERMAN, M. L. BLEIBERG, and W. YENIS-CAVICH, *J. Nucl. Mater.*, **2**, 129 (1960).

41. H. MATZKE and J. L. WHITTON, *Can. J. Phys.*, **44**, 995 (1966).

42. J. CAMERON, University of Wisconsin, Private Communication (1974).

43. W. W. ENGEL, Jr., "A User's Manual for ANISN," K-1693, Oak Ridge Gaseous Diffusion Plant (1967).

44. R. Q. WRIGHT et al., "SUPERTOG: A Program to Generate Fine Group Constants and P_n Scattering Matrices from ENDF/B," ORNL-TM-2679, Oak Ridge National Laboratory (1969).

45. J. R. KNIGHT and F. R. MYNATT, "MUG, A Program for Generating Multigroup Photon Cross Sections," CTC-17, Computing Technology Center, Union Carbide Corporation (1970).

46. M. K. DRAKE, Ed., "Data Formats and Procedures for the ENDF Neutron Cross Section Library," BNL-50279, Brookhaven National Laboratory (1970).

47. D. J. DUDZIAK et al., "LAPHANO: A Po Mutigroup Photon-Production Matrix and Source Code for ENDF," LA-4750-MS, Los Alamos Scientific Laboratory (1972).

48. M.A. ABDOU, C.W. MAYNARD, and R.Q. WRIGHT, "MACK: A Computer Program to Calculate Neutron Energy Release Parameters (Fluence-to-Kerma Factors) and Multigroup Neutron Cross Sections from Nuclear Data in ENDF Format," UWFDM, University of Wisconsin (1973); also issued as ORNL-TM-3994, Oak Ridge National Laboratory (1973).

49. M. A. ABDOU, "Calculational Methods for Nuclear Heating and Neutronics and Photonics Design for CTR Blanket and Shields," PhD Thesis, 74-8981, University Microfilms, Inc.; also issued as UWFDM-66 and UWFDM-67, University of Wisconsin, Nuclear Engineering Department (1973).

50. W. J. GRAY and W. C. MORGAN, "Projection of Graphite Behavior: Comparison of Results for Four Conceptual Fusion Reactor Designs," to be published.

51. R. W. CONN, G. L. KULCINSKI, M. A. ABDOU, R. W. BOOM, G. EMMERT, Y. EYSSA, M. HILAL, J. KESNER, W. LUE, C. MAYNARD, A. MENSE, J. SCHARER, T. SUNG, I. SVIATOSLAVSKY, D. SZE, W. VOGELSANG, L. WITTENBERG, T. YANG, and W. YOUNG, "Major Design Features of the Conceptual D-T Tokamak Power Reactor, UWMAK-I," *Proc. 5th IAEA Conf. Plasma Physics and Controlled Nuclear Fusion Research*, Tokyo, Japan, November 11-15, 1975. To be published.

52. M. A. ABDOU and C. W. MAYNARD, "Nuclear Design of the Magnet Shield for Fusion Reactors," *Proc. 1st. Topl. Mtg. Technology of Controlled Nuclear Fusion*, CONF-740402-P1, U.S. Atomic Energy Commission (1974).

53. V. A. MARONI, "An Analysis of Tritium Distribution and Leakage Characteristics for Two-Fusion Reactor Reference Designs," CEN/CTR/TM-9, Argonne National Laboratory (1974).

54. Linde Molecular Sieves Data Sheet, Union Carbide Corporation, New York (1974).